tTEM20AAR: a benchmark geophysical dataset for unconsolidated fluvio-glacial sediments

Alexis Neven[1]**, Pradip K. Maurya**[2]**, Anders Vest Christiansen**[2]**, and Philippe Renard**[1,3]

[1]Centre of Hydrogeology and Geothermics, University of Neuchâtel, Neuchâtel, Switzerland
[2]Department of Earth Sciences, Aarhus University, Aarhus C, Denmark
[3]Department of Geosciences, University of Oslo, Oslo, Norway
[*]corresponding author: Alexis Neven (alexis.neven@unine.ch)

ABSTRACT

Quaternary deposits are complex and heterogeneous. They contain some of the most abundant and extensively used aquifers. In order to improve the knowledge of the spatial heterogeneity of such deposits, we acquired a large (1500 hectares) and dense (20m spacing) Time Domain ElectroMagnetic (TDEM) dataset in the upper Aare Valley, Switzerland. TDEM is a fast and reliable method to measure the magnetic field directly related to the resistivity of the underground. In this paper, we present the inverted resistivity models derived from this acquisition. The depth of investigation ranges between 40 to 120m depth, with an average data residual contained in the standard deviation of the data. These data can be used for many different purposes: from sedimentological interpretation of quaternary environments in alpine environments, geological and hydrogeological modeling, to benchmarking geophysical inversion techniques.

Background & Summary

In most urbanized and agricultural areas of Switzerland, the shallow underground is constituted of Quaternary deposits. The thickness can vary from few meters to hundreds of meters. These recent sediments are deposited by various agents such as rivers, lakes, glaciers or even landslides. Each time, the associated sediment will have a different composition and permeability and a spatial variability that is often higher than expected in such deposits.

However, these formations are some of the most solicited: water supply for cities, extraction of construction materials and shallow geothermal exploitation. Often, the construction of geological models using only boreholes can miss most of the spatial heterogeneity, and lead to inadequate models and wrong conclusions. Increasing the number of boreholes to reduce the uncertainty is often difficult and expensive. A good example of these highly exploited Quaternary zones is the upper Aare Valley. (fig. 1). In 60 km^2, the Aare Valley includes 4 quarries, 6350 pumping wells (Shallow geothermic or drinkable water) and 5300 injection wells (re-inject water after geothermal heat pump). A previous valley size model was designed using boreholes and surface data[1], but the model does not represent the internal heterogeneities of the Quaternary formations and can show unrealistic sharp variations due to the nearest neighbors interpolation method used during the workflow. Therefore, there is a need for a better understanding of Quaternary sedimentary heterogeneity, in order to better constrain geological models, knowledge that could be applied in the Aare valley or for any fluvio-glacial filling area.

Near-surface geophysics such as DC resistivity, electromagnetic or seismic methods can bring important information in terms of the spatial distribution of facies. However, they are usually carried out in restricted areas to answer specific local questions, and do not help to understand the variations of

geology at the valley scale. In order to fill this gap of information, and provide a valley scale fluvio-glacial resistivity map, we conducted in January 2020 a large geophysical survey using tTEM (towed Transient Electromagnetic) system[2] in the upper Aare Valley, Switzerland. The tTEM-system provides a very detailed (both vertically and horizontally) resistivity model. The *tTEM20AAR* dataset covers a section of the valley of approximately 1-2 km width and 16 km long. The fields were mapped with a line spacing of 20 meters, resulting in about 1500 hectares of covered land (see fig. 1). The raw tTEM data were processed to suppress noisy data parts, and then inverted to a resistivity model using spatially constrained inversion algorithm[3]. The resulting resistivity model consists of 57'862 1D models of 30 layers. The depth of investigation varies, from 40 to 120 meters depth, primary driven by lithological/resistivity variations. The resulting resistivity model explains (fits) the recorded data well within the estimated data uncertainty. The resistivity model reveals new and very interesting geophysical/geological structures of the subsurface at a fine resolution. At a first sight, they seem to reveal possible paleo river channels, various stages of glacial advances and retreat, as well as landslide lateral deposits. These structures still require a more detailed analysis and geological interpretation. Example of geological interpretations of such data are available in[4].

The *tTEM20AAR* data set can be used for several purposes. It can be used as a benchmark to test and compare geophysical inversion procedures for tTEM-systems. Stochastic inversion[5,6] using different methods or types of prior knowledge could also be applied on this data set and be compared with the published results. In addition, if other geophysical data are acquired on the same site in the future, they could complement the analysis by performing joint inversion. More generally, quaternary formations are highly heterogeneous and constitute a challenge for geostatistical and uncertainty modeling[7]. Sharing this dataset will allow to test and compare various methods to interpolate the properties of the underground and construct models that can be used for various purposes. The integration of geophysical methods to constrain hydrogeological models is also a very important field of research[8]. The *tTEM20AAR* data set may help testing the development of innovative methods for the construction of groundwater models. It is important to note in this perspective that the Upper Aare Valley has been extensively studied and a consequent amount of additional data are distributed by the Swiss authorities. Improvement in data integration may strongly improve hydrogeological modeling in such environments, subject to high local facies variations.

Finally, from a more geological perspective, the *tTEM20AAR* data set could be used to better understand the internal structures of quaternary deposits within alpine valleys. It could be analysed in detail from a sedimentological perspective and used to better constrain the glacial and geological history of the quaternary deposits[9].

Methods

The tTEM-system

The tTEM-system used for the data acquisition is developed by the HGG-group at Aarhus University, Denmark[2]. The tTEM-system is a towed, ground-based, transient electromagnetic system, designed for highly efficient data collection and detailed 3D-mapping of the shallow subsurface (the upper 80 m). TEM-methods build on the principle of induction (Faraday's law of induction) for mapping the electrical conductivity (conductivity=1/resistivity) of the subsurface. A detailed description of the TEM principle can be found in[10]. The layout of the tTEM-system is shown in Figure 2.

The tTEM-system consists of an All-Terrain Vehicle (ATV) carrying the instrumentation and towing the transmitter frame (Tx coil) and the receiver coil (Rx coil) in an offset configuration. The Tx and Rx coils are mounted on sleds for all terrain capability. All frame parts and sleds are built of non-conductive
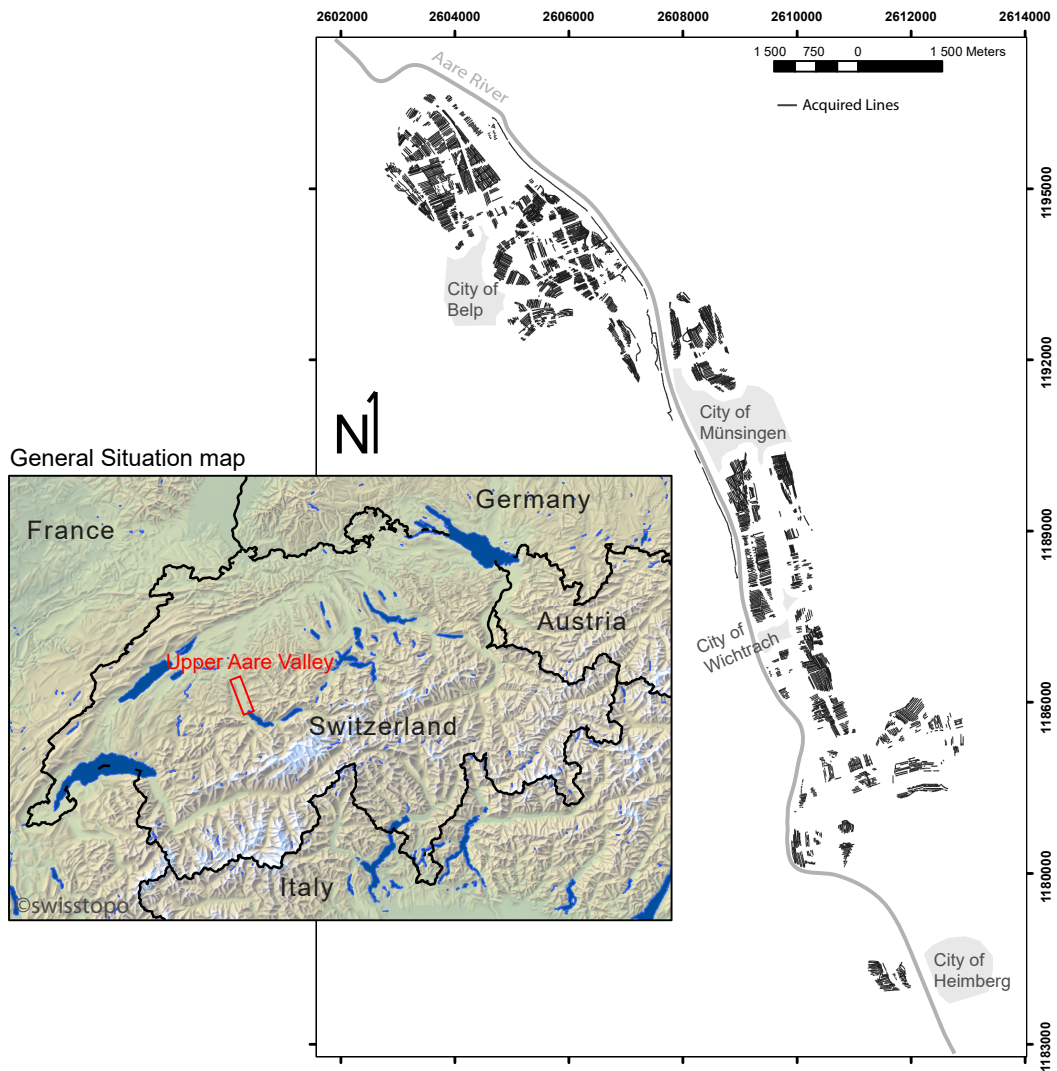
Figure 1. Location of the study area and acquisition lines. Coordinates are in UTM 32N.

composite materials. Driving path and various data quality control parameters are monitored in real time by the driver on a mounted screen. Operation speed is up to 20 km/h. We used an off-set configuration, where the receiver coil is 7 meters behind the transmitter coil. Both of them are horizontal, allowing to measure the z component of the secondary magnetic field. A GPS is mounted on the frame to ensure correct positioning of the data. The transmitter loop consists of one loop of 4x2 m, creating an area of 8 m^2. We used a standard dual moment TEM configuration: a high moment (HM) with a high inductive current of 30 A and a low moment with a lower inductive current of 5 A. Such configuration has the advantage of being able to resolve shallow targets with the low moment and its associated fast turn off time, and to reach higher penetration depth with the high moment. Both moments are stacked few hundreds times. Detailed parameters are summarized in the table 1. The gate is the time interval in which the received amplitudes are averaged. Due to the signal attenuation, further we get in the listening time, lower is the signal to noise ratio. In order to partially counterbalance this effect, we used a logarithmic increasing gate size related to listening time.

   To ensure the data quality, the tTEM-instrumentation were calibrated prior to the survey at the Danish national TEM test site following the calibration procedure described by[11]. The two calibrated parameters
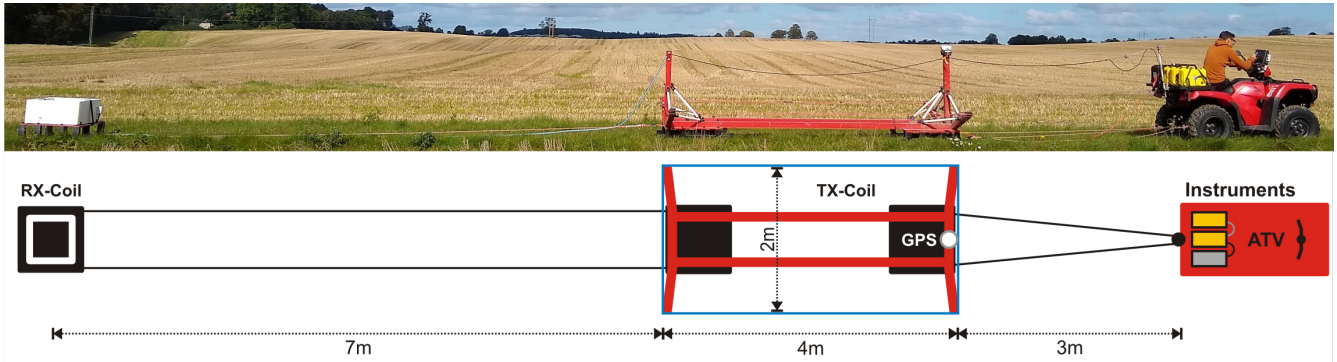
Figure 2. The tTEM-system.

Parameters	LM	HM
Tx No. of turn		1
Tx coil area		8 m^2
Transmitter current	5 A	30 A
Peak moment	30 Am^2	240 Am^2
Repetition frequency	1055 Hz	315 Hz
Stacks	422	252
Total cyclus time	0.22 s	0.40 s
Tx time	0.2 ms	0.45 ms
Turn off time	2.8 μ s	4.5 μ s
Number of gates	4	23
Gate size	4 μ s - 10 μ s	10 μ s - 900 μ s
First gate start	4.38 μ s	10.30 μ s

Table 1. Specifications of the High and Low moment used in the acquisition. The gate size increases with time in order to counterbalance less good signal to noise ratio due to the wave attenuation.
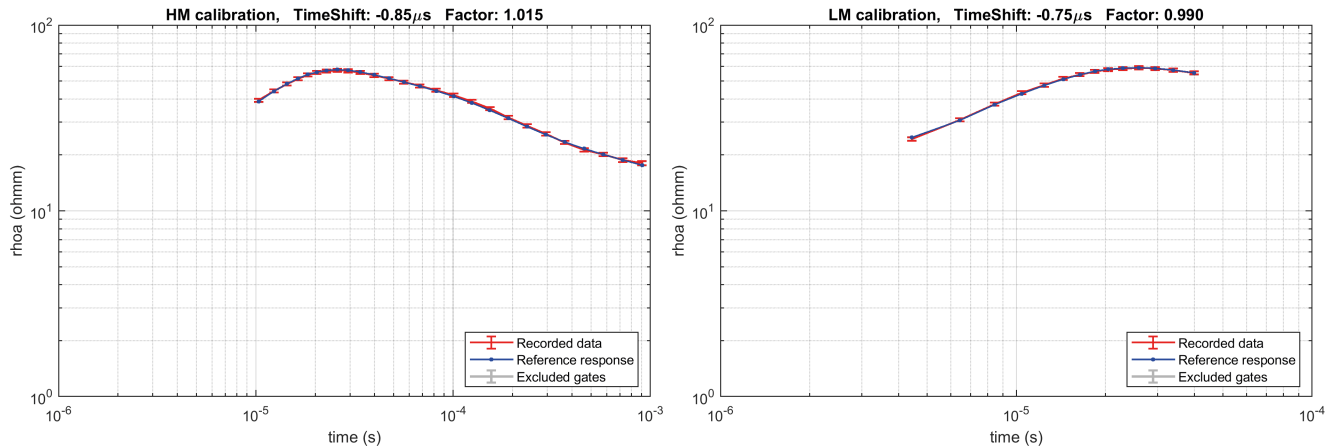
Figure 3. Calibration of the High and Low moment. The resulting time shift and scale factor are respectively -0.75 μs and 0.99 for the LM, and - 0.85 μs and 1.015 for the HM.

are a time shift and an amplitude factor. The calibration was done with the ATV connected to the equipment in order to account for any shift caused by it. Figure 3 shows the match between the test site reference response and the measured tTEM-response after calibration, which results in a fully acceptable match.

Field Site

The field site is the Upper Aare Valley, in central Switzerland (see figure 1). The survey took place in January 2020. During approximately 15 working days, we covered all the accessible farming fields in the valley along a 26 km long section. The driving speed was between 10 to 20 km/h, depending of the terrain. Since the acquisition rate is time dependant, and not distance triggered, we also lowered the speed in noisier or less responsive areas in order to acquire a denser dataset. The spacing between the lines was approximately 20 meters. The average covered surface par day was 112 hectares, for a total of 1425 hectares.

Data Processing

The voltage data from the receiver is measured continuously, and need to be cleaned of man-made noise and coupling. Data processing and inversion were carried out with the tTEM processing module in the *Aarhus Workbench* software. The objective of the processing of the tTEM-data is to remove any interference in the data from man-made installation (coupled data), suppress random noise by stacking, and finally discard the noisy late time data entering the background noise. Thus, we ensure that the resulting resistivity model represents geological structures of the subsurface without artifact from man-made installation. Processing of the dB/dt data comprises of the following steps:

- Automatic detection of capacitive coupling pattern in the raw data using slope filter as coupling appears as abrupt slope changes in a sounding curve.

- Averaging of raw data to suppress random noise. Raw data are averaged using a moving average filter with narrow time windows in early times and wider in the late times.

- Creation of vertical soundings every 2.5 s which corresponds approximately to a spacing of 10 m. The exact distance can vary depending on driving speed.

- Automatic filtering of the averaged data for removal of late-time data points entering the background noise.

- Visual assessment of all dB/dt data and manual removal of coupled data not detected by the automatic filtering and validation of automatically detected couplings.

- Evaluation and adjustment of the data processing based on preliminary inversion results.

Furthermore GPS data are lag-corrected to geographical positioned data/models at center between transmitter and receiver coils. The data uncertainty consists of a minimum of 3% as uniform data standard deviation (STD) plus the STD calculated from the data stacking. Averaged data resulting with STD over 30% are discarded from inversion.

Inversion

The electrical resistivities of the underground are then estimated using a series of 3D constrained 1D-inversions. The 1D inversion is based on the *AarhusInv* code[12, 13]. This code is an implementation of a 1D non-linear damped least-squares solution, with a modeled transfer function for the TEM instrumentation. This function takes into account the transmitter waveform, the instrument low pass filters, the receiver bandwidth, the system geometry, the gate widths and the instrument front gate. However, in such an standalone 1D inversion, each model is totally independent of the neighboring ones. To account for the lateral continuity expected in geological environments, the spatially constrained inversion (SCI)[3] method was used. It applies 3D constraints to 1D inversion models both along and across the mapping lines, with a weight that is decreasing with distance. All the inversions were carried out with the *Aarhus Workbench* software.

The SCI inversion can be used with two different schemes of regularization: smooth or sharp. The smooth scheme tends to minimize abrupt changes in resistivity, in the vertical and horizontal directions. On the other hand, the sharp regularization scheme tends to minimize the number of resistivity changes, but will consequently result in more abrupt resistivity transitions and a potential more blocky model appearance. Both regularizations were used, and are included in the output data.

For each resistivity model, we estimate the depth of investigation (DOI) using a method based on the Jacobian Sensitivity matrix[14]. This method has the advantage of taking into account the full transfer function, including system geometry, data uncertainty and the resistivity model. Two DOI thresholds values in the sensitivity matrix were used to provide the reported DOI-standard, and the DOI-conservative values. As a guideline, the resistivity structures above the DOI-conservative value are strongly data driven, while resistivity structures below the DOI-standard value are weakly represented in the data. Normally one would blank the resistivity models below DOI-standard value. In addition, the shallowest resolution of the tTEM system is 2 to 3 m , depending of the resistivity.

Inversion setup for the smooth and sharp inversions are summarized in the table 2. The figure 4 presents some resistivity maps data extracted from the smooth regularization inversion. In addition, the same cross section across the north area from the sharp and the smooth regularization is displayed. Both DOI are also outlined for comparison. The spatial variations of the Quaternary deposits, in both depth intervals and cross-section are clearly visible. Such variations in resistivities also indicates variations in lithologies, and therefore variations in hydrological proprieties.

Data Records

After the data processing and the inversion, the processed data, the resistivity models and the associated forward responses from the smooth and sharp inversions had been produced. These data[15] are provided in
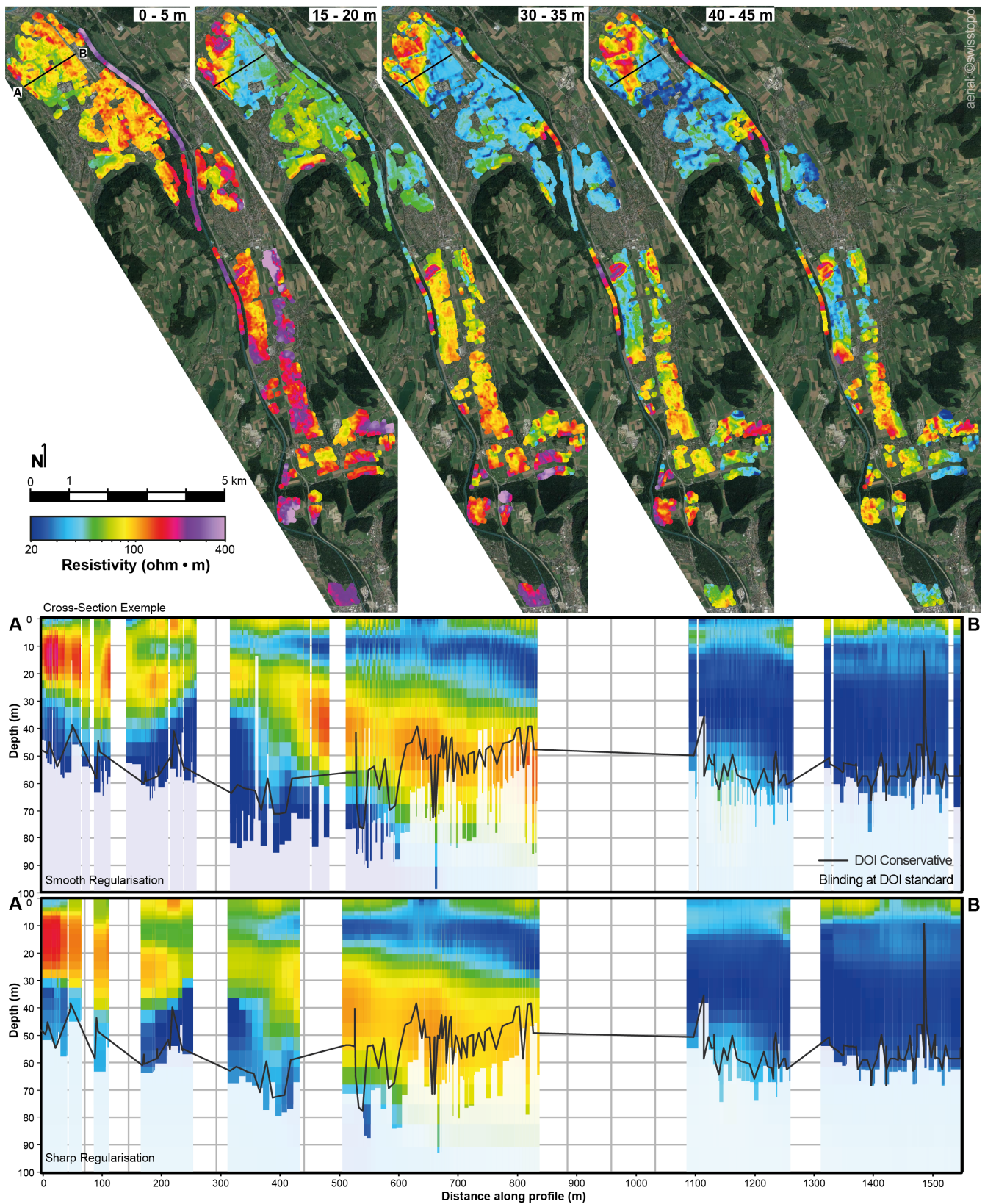
Figure 4. Top : Mean resistivity maps at different depth intervals from the smooth regularization model. Bottom : NE-SW cross section with different regularizations. The models are blinded at the DOI-standard, and the black line represent the DOI-conservative. Base map from Swiss Federal Topographic Office

Item	Parameter	Value
Model Setup	Number of layers	30
	Model resistivity start value (uniform - no prior)	40 ohmm
	Thickness of first layer (m)	1 m
	Depth to last layer (m)	120 m depth
	Thickness of layers	Log increasing with depth
Smooth Constraints	Factor of horizontal contrains on resistivites	1.5
	Factor of vertical contrains on resistivites	2.0
	Reference distance	10 m
	SCI Constraints with distance	$1/distance^{0.75}$
	Prior, thickness	Fixed
	Prior, resistivities	None
	Minimum number of gates per inversion point	2
Sharp Constrains	Factor of horizontal contrains on resistivites	1.12
	Factor of vertical contrains on resistivites	1.08
	Reference distance	10 m
	SCI Constraints with distance	$1/distance^{0.75}$
	Prior, thickness	Fixed
	Prior, resistivities	None
	Minimum number of gates per inversion point	2
	Sharp vertical constrains	500
	Sharp horizontal constrains	300

Table 2. Settings used for the model setup, the smooth and the sharp regularization.

Processed_Data.dat			
Column	Label	Unit	Description
1	RECORD		Global record number. Links the data to the resistivity model in the `*.inv` files
2	LINE_NO		Line number (Line number 0 = data/model not tacked with a line number)
3	UTMX	(m)	UTMX coordinate, WGS 84 UTM zone 32N (epsg:32632)
4	UTMY	(m)	UTMY coordinate, WGS 84 UTM zone 32N (epsg:32632)
5	ELEVATION	(m)	Surface elevation
6	NUMDATA		Number of data points (gates) in-use for the segment/sounding
7	SEGMENT		Transmitter moment indicator. 1=Low moment, 2=High moment
8-37	DATA_#	(V/(Am4))	Processed z-component dB/dt data value for gate number #. 9999 values = data not in-use/not present
38-66	DATASTD_#	STD	Data uncertainty for DATA_#, stated as a relative STD in log space.

Table 3. Structure of the .dat data file

157 column based ASCII files. Each file structure is outlined in the following sections.

158 **Processed data file**

The `Processed_Data.dat` file contains the processed tTEM data and data uncertainties. Each line in the file corresponds to a low moment (LM) or high moment (HM) data stack for a given location. The RECORD number links the LM and HM data to a given resistivity model in the `*.inv` files. Number 9999 marks discarded data points or data points not present for the given moment. If all the data points of LM or HM are discarded then the data line is not present in the file. Gate center time and other info is stated in the header lines. The data uncertainty is given as relative in log space. The upper and lower bounds of the data are then defined as :

$$\text{unc}_{\text{down}} = \frac{\text{DATA}}{1 + \text{DATASTD}} \tag{1}$$

$$\text{unc}_{\text{up}} = \text{DATA} \times (1 + \text{DATASTD}) \tag{2}$$

159 with unc_{down} and unc_{up} being the absolute lower and upper uncertainties, DATA the processed z-
160 component dB/dt data value and DATASTD the relative uncertainty. The structure is outlined in the
161 following table 3.

162 **Inversion Model File**

163 The `Sharp_Model.inv` and `Smooth_Model.inv` files contain the resistivity models (layer resistiv-
164 ity and layer thicknesses). Each line hold a 30-layers resistivity model. The RECORD links the model to
165 the data in the process data and forward data files. The file also contains the DOI, and the data fit. Note
166 that the last layer (layer 30) does not have a thickness since it continues to infinite depth in the modeling.
167 Normally, the DOI-standard values are used to blank the models in depths. The detailed file structure is
168 provided in table 4.

Smooth_Model.inv, Sharp_Model.inv			
Colum	Label	Unit	Description
1	RECORD		Global record number. Links the model the data in the *.inv files
2	LINE_NO		Line number (Line number 0 = data/model not tacked with a line number)
3	UTMX	(m)	UTMX coordinate, WGS 84 UTM zone 32N (epsg:32632)
4	UTMY	(m)	UTMY coordinate, WGS 84 UTM zone 32N (epsg:32632)
5	ELEVATION	(m)	Surface elevation
6	DATAFIT		Data fit (Data residual)
7-36	RHO_I_#	(Ohmm)	Resistivity of layer#.
37-65	THK_#	(m)	Thickness of layer #.
66	DOI_CONSERVATIVE	(m)	Estimated depth of investigation, conservative threshold value used
67	DOI_STANDARD	(m)	Estimated depth of investigation, standard threshold value used

Table 4. Structure of the *.inv datafile

Synthetic response file

The `Forward_Data_Sharp.dat` and `Forward_Data_Smooth.dat` files contains the forward responses of the sharp and smooth resistivity models. The structure of the forward data files is the same as the `Processed_Data.dat` file except that the forward responses does not have associated data uncertainties. Detailed file structure is provided in table 5.

Technical Validation

After the removal of coupled structures, the main indicator of geophysical data quality is the fit with the inverted model. In case of error in the data, such as undetected coupling for example, the data will not be fitted by any plausible resistivity model and will present an important residual error. Therefore, a good fit between the theoretical forward response and the field data indicates that the data are representative of the geology and not affected by errors or noise.

The quality of inversion is assessed by a quality control parameter called data misfit. We compare the forward geophysical response of our final resistivity model, with the field data, normalized by the square of the standard deviation of our data. The indicator is defined by the following equation 3.

Forward_Data_Smooth.dat, Forward_Data_Sharp.dat			
Column	Label	Unit	Description
1	RECORD		Global record number. Links the data to the resistivity model in the `*.inv` files
2	LINE_NO		Line number (Line number 0 = data/model not tacked with a line number)
3	UTMX	(m)	UTMX coordinate, WGS 84 UTM zone 32N (epsg:32632)
4	UTMY	(m)	UTMY coordinate, WGS 84 UTM zone 32N (epsg:32632)
5	ELEVATION	(m)	Surface elevation
6	NUMDATA		Number of data points (gates) in-use for the segment/sounding
7	SEGMENT		Transmitter moment indicator. 1=Low moment, 2=High moment
8-37	DATA_#	(V/(Am4))	Model forward response, dB/dt, for gate number #. 9999 values = data not in-use/not present

Table 5. Structure of the *.syn data file
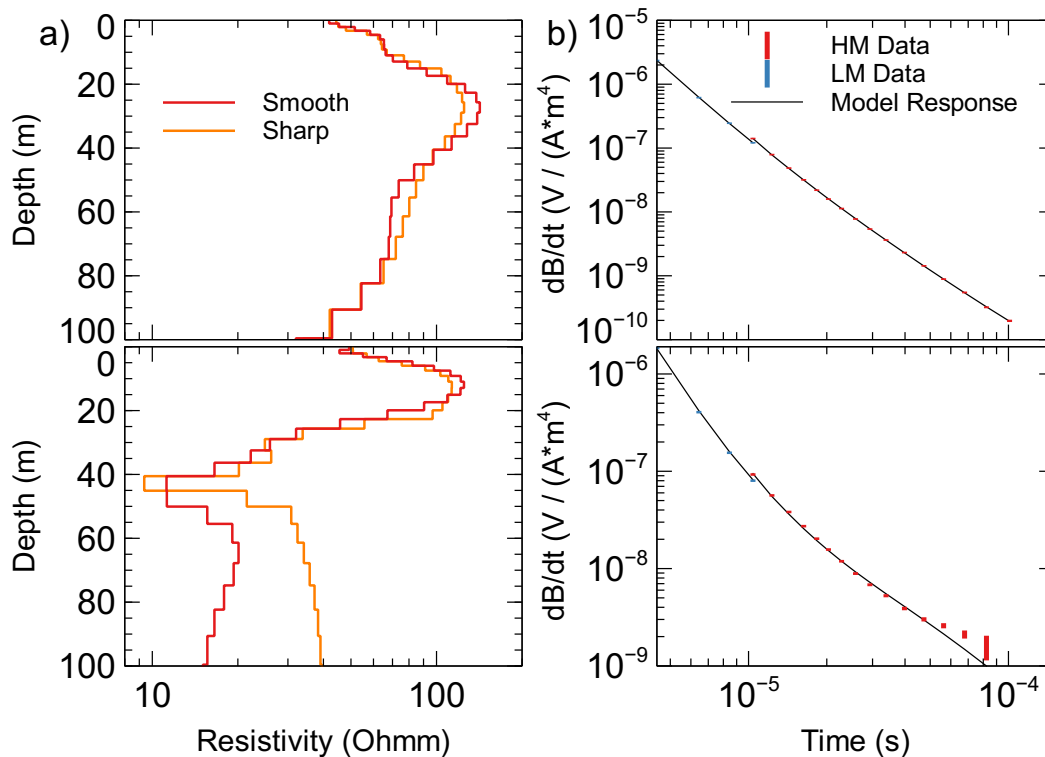
Figure 5. Example of two 1D model at a location, the top one considered as undisturbed and the bottom one as a noisy sounding. Top : Number 44384 on line 20350 at position 384744.1875/5196856 UTM 32 N. Bottom : Number 38407 on line 17610 at position 384313/5195797. a) Resistivity models for two regularizations. b) associated forward response of the smooth model in black, with the LM & HM data point with red & blue error bars. The normalized data fit (see text) for the top model/data curve is 0.27 and 1.36 for the bottom model.

$$\text{Data Misfit} = \sqrt{\frac{1}{N}\sum_{i=1}^{N}\frac{(d_{obs,i}-d_{frw,i})^2}{\sigma_{d,i}^2}} \tag{3}$$

where d_{obs} is the observed data, d_{fwr} is the forward data, σ_d is the uncertainty of the observed data and N is the total number of data point.

A data residual below 1 indicates that our final model response is within one standard deviation of the data, when a value above 1 indicates a response out of one standard deviation. Figure 5b shows, a single data curve (error bars) and the forward response (line) from the resistivity models in figure 5a. Both regularization are shown. The first model (top figure) is situated in the middle of a field, when
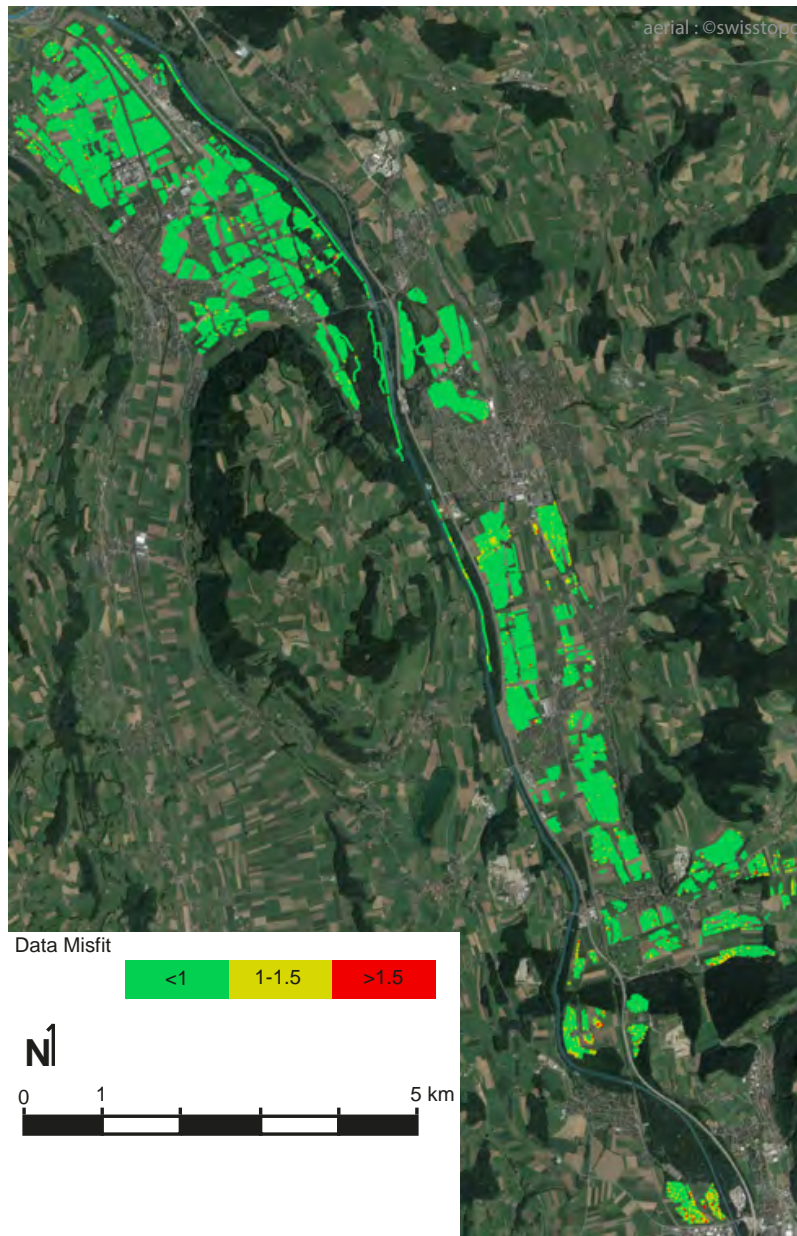
Figure 6. Data Misfit over the acquisition area. Base map from Swiss Federal Topographic Office.

the second model (bottom figure) is close to a road, which is a typical source for electromagnetic noise. The associated data-misfit for the first model is 0.27, and 1.36 for the noisier one. Most of the misfit comes from the latest's gates, when the signal to noise ratio is getting small. The data misfit for the all smooth inversion models is plotted in Figure 6. As seen in figure 6, the data misfit is in general well below one and fully acceptable. 95% of the data is within 1 standard deviation, with a global misfit average of 0.65 and 0.52 respectively for the sharp and smooth models. A manual inspection of the high data misfit models revealed that they are all associated to highly resistive models, and/or are close to man made electromagnetic noise such as roads, fences, or train tracks. A good example is the extreme south of the acquisition, that is one of the most resistive areas. This situation logically leads to a lower signal to noise ratio, and due to the spatial constraints of the inversion, it will consequently leads to an higher data misfit. However, they are usually restricted to only a few local data-points, and the models are similar to neighbouring ones that has acceptable misfit. We therefore decided to keep them in the dataset.

Finally, users of the data should be aware that the footprint of the equipment is at least 9m at the surface (size of the equipment) and is increasing with depth and wave diffusion. Consequently, a sharp vertical transition in the geology for example, will tend to appear oblique in the resistivity data due to this effect. The resistivity models proposed here are only the one that fits the best our data.

Usage Notes

Since the file data format is a standard ASCII file, all the files can be used with any program supporting xzy format.

Code availability

All the data importation, processing and SCI inversions were done using *Aarhus Workbench* commercial software developed by *Aarhusgeosoftware*. The 1D inversion code used is *AarhusInv* developed by the Aarhus University Hydrogeophysics group[12, 13]. The *AarhusInv* code is free to use for research purpose.

References

1. Volken, S., Preisig, G. & Gaehwiler, M. Geoquat: Developing a system for the sustainable management, 3D modelling and application of quaternary deposit data. *Swiss Bull. for Appl. Geol.* **21**, 3–16, 10.5169/seals-658182 (2016).

2. Auken, E. *et al.* tTEM — a towed transient electromagnetic system for detailed 3d imaging of the top 70 m of the subsurface. *GEOPHYSICS* **84**, E13–E22, 10.1190/geo2018-0355.1 (2019).

3. Viezzoli, A., Christiansen, A. V., Auken, E. & Sørensen, K. Quasi-3d modeling of airborne TEM data by spatially constrained inversion. *GEOPHYSICS* **73**, F105–F113, 10.1190/1.2895521 (2008).

4. Sandersen, P. B. *et al.* Utilizing the towed transient ElectroMagnetic method (tTEM) for achieving unprecedented near-surface detail in geological mapping. *Eng. Geol.* 106125, 10.1016/j.enggeo.2021.106125 (2021).

5. Mosegaard, K. & Tarantola, A. Monte Carlo sampling of solutions to inverse problems. *J. Geophys. Res. Solid Earth* **100**, 12431–12447, 10.1029/94JB03097 (1995).

6. Linde, N., Ginsbourger, D., Irving, J., Nobile, F. & Doucet, A. On uncertainty quantification in hydrogeology and hydrogeophysics. *Adv. Water Resour.* **110**, 166–181, 10.1016/j.advwatres.2017.10.014 (2017).

7. De Marsily, G. *et al.* Dealing with spatial heterogeneity. *Hydrogeol. J.* **13**, 161–183, 10.1007/s10040-004-0432-3 (2005).

8. Binley, A. *et al.* The emergence of hydrogeophysics for improved understanding of subsurface processes over multiple scales. *Water resources research* **51**, 3837–3866, 10.1002/2015WR017016 (2015).

9. Preusser, F., Graf, H. R., Keller, O., Krayss, E. & Schlüchter, C. Quaternary glaciation history of northern switzerland. *E&G Quat. Sci. J.* **60**, 282–305, 10.3285/eg.60.2-3.06 (2011).

10. Christiansen, A. V., Auken, E. & Sørensen, K. The transient electromagnetic method. In Kirsch, R. (ed.) *Groundwater Geophysics: A Tool for Hydrogeology*, 179–226, 10.1007/978-3-540-88405-7_6 (Springer Berlin Heidelberg, Berlin, Heidelberg, 2009).

11. Foged, N., Auken, E., Christiansen, A. V. & Sørensen, K. I. Test-site calibration and validation of airborne and ground-based TEM systems. *GEOPHYSICS* **78**, E95–E106, 10.1190/geo2012-0244.1 (2013).

12. Auken, E. *et al.* An overview of a highly versatile forward and stable inverse algorithm for airborne, ground-based and borehole electromagnetic and electric data. *Explor. Geophys.* **46**, 223–235, 10.1071/eg13097 (2015).

13. Kirkegaard, C. *et al.* Utilizing massively parallel co-processors in the AarhusInv 1d forward and inverse AEM modelling code. *ASEG Ext. Abstr.* **2015**, 1–3, 10.1071/aseg2015ab125 (2015).

14. Christiansen, A. V. & Auken, E. A global measure for depth of investigation. *GEOPHYSICS* **77**, WB171–WB177, 10.1190/geo2011-0393.1 (2012).

15. Neven, A., Pradip K. Maurya, Christiansen, A. V. & Renard, P. tTEM20AAR: a tTEM geophysical dataset, 10.5281/ZENODO.4269887 (2020).

Acknowledgements

The data set described in this paper was acquired within the framework of the Phenix project funded by the Swiss National Science foundation under the grant number 182600. The authors are thankful to all the people who contributed to the data acquisition and its inversion, and in particular: Rune Kraghede, Jesper Bjergsted Pedersen, Nikolaj Foged, Lucile Chauveau, Ilias Ben Ammar, Cyprien Louis as well as the local authorities and numerous farmers who provided access to their fields for the survey.

Author contributions statement

A.N. coordinated, conducted and supervised the field work. He performed the data analysis and inversion, prepared the data and wrote the paper. A.V.C. and P.M provided the instruments and software. They participated in the design of the measurements and checked the quality of data treatment and inversion. They edited and corrected the manuscript. P.R. obtained the funding for the survey. He supervised the work, participated to the field acquisition, and was involved in the data preparation, writing, and editing of the paper.

Competing interests

The authors declare no conflicts of interests.